Title

Liquefaction of Semen Generates and Later Degrades a Conserved Semenogelin Peptide That Enhances HIV Infection

Journal

Journal of Virology, 88(13)

ISSN

0022-538X

Authors

Roan, Nadia R
Liu, Haichuan
Usmani, Shariq M
et al.

Publication Date

2014-07-01

DOI

10.1128/jvi.00269-14

Peer reviewed

JVI Journals.ASM.org

Liquefaction of Semen Generates and Later Degrades a Conserved Semenogelin Peptide That Enhances HIV Infection

Nadia R. Roan,[a,b] Haichuan Liu,[c] Shariq M. Usmani,[d] Jason Neidleman,[a] Janis A. Müller,[d] Aram Avila-Herrera,[e] Ali Gawanbacht,[d] Onofrio Zirafi,[d] Simon Chu,[a] Ming Dong,[f] Senthil T. Kumar,[g] James F. Smith,[b] Katherine S. Pollard,[e,h] Marcus Fändrich,[g] Frank Kirchhoff,[d] Jan Münch,[d] H. Ewa Witkowska,[c] Warner C. Greene[a,i]

Gladstone Institute of Virology and Immunology,[a] Department of Urology,[b] Department of Obstetrics, Gynecology & Reproductive Sciences and Sandler-Moore Mass Spectrometry Core Facility,[c] Gladstone Institute of Cardiovascular Diseases,[e] Department of Epidemiology and Biostatistics, Institute for Human Genetics,[h] and Departments of Medicine and Microbiology and Immunology,[i] University of California, San Francisco, California, USA; Institute of Molecular Virology, Ulm University Medical Center, Ulm, Germany[d]; Lawrence Berkeley National Laboratory, Berkeley, California, USA[f]; Institute of Pharmaceutical Biotechnology, Ulm University, Ulm, Germany[g]

ABSTRACT

Semen enhances HIV infection *in vitro*, but how long it retains this activity has not been carefully examined. Immediately postejaculation, semen exists as a semisolid coagulum, which then converts to a more liquid form in a process termed liquefaction. We demonstrate that early during liquefaction, semen exhibits maximal HIV-enhancing activity that gradually declines upon further incubation. The decline in HIV-enhancing activity parallels the degradation of peptide fragments derived from the semenogelins (SEMs), the major components of the coagulum that are cleaved in a site-specific and progressive manner upon initiation of liquefaction. Because amyloid fibrils generated from SEM fragments were recently demonstrated to enhance HIV infection, we set out to determine whether any of the liquefaction-generated SEM fragments associate with the presence of HIV-enhancing activity. We identify SEM1 from amino acids 86 to 107 [SEM1(86-107)] to be a short, cationic, amyloidogenic SEM peptide that is generated early in the process of liquefaction but that, conversely, is lost during prolonged liquefaction due to the activity of serine proteases. Synthetic SEM1(86-107) amyloids directly bind HIV-1 virions and are sufficient to enhance HIV infection of permissive cells. Furthermore, endogenous seminal levels of SEM1(86-107) correlate with donor-dependent variations in viral enhancement activity, and antibodies generated against SEM1(86-107) recognize endogenous amyloids in human semen. The amyloidogenic potential of SEM1(86-107) and its virus-enhancing properties are conserved among great apes, suggesting an evolutionarily conserved function. These studies identify SEM1(86-107) to be a key, HIV-enhancing amyloid species in human semen and underscore the dynamic nature of semen's HIV-enhancing activity.

IMPORTANCE

Semen, the most common vehicle for HIV transmission, enhances HIV infection *in vitro*, but how long it retains this activity has not been investigated. Semen naturally undergoes physiological changes over time, whereby it converts from a gel-like consistency to a more liquid form. This process, termed liquefaction, is characterized at the molecular level by site-specific and progressive cleavage of SEMs, the major components of the coagulum, by seminal proteases. We demonstrate that the HIV-enhancing activity of semen gradually decreases over the course of extended liquefaction and identify a naturally occurring semenogelin-derived fragment, SEM1(86-107), whose levels correlate with virus-enhancing activity over the course of liquefaction. SEM1(86-107) amyloids are naturally present in semen, and synthetic SEM1(86-107) fibrils bind virions and are sufficient to enhance HIV infection. Therefore, by characterizing dynamic changes in the HIV-enhancing activity of semen during extended liquefaction, we identified SEM1(86-107) to be a key virus-enhancing component of human semen.

Human semen is a complex biological fluid that begins as a gelatinous structure and, over time, undergoes regulated changes in consistency in a process termed liquefaction. Immediately upon ejaculation, it forms a viscous gel referred to as the coagulum. The major components of the coagulum are semenogelin 1 (SEM1) and SEM2, highly abundant proteins present at concentrations up to 20 mg/ml in seminal fluid (SF) (1). SEMs are produced by the seminal vesicles and mixed with secretions from other male sex glands immediately prior to semen emission. During liquefaction, the coagulum transforms into a more fluid-like material due to site-specific and progressive proteolytic cleavage of the SEMs by prostate-specific antigen (PSA) (2–5). The molecular basis of how the SEMs polymerize to form the coagulum is not clear (1), and indeed, the precise function of the coagulum is debated (6, 7).

We recently showed that amyloids derived from SEM fragments promote HIV infection. Through the use of an amyloid-specific antibody, we identified SEM peptides that can self-assemble into amyloid fibrils that enhance HIV attachment to target

Received 13 February 2014 **Accepted** 7 April 2014
Published ahead of print 16 April 2014
Editor: B. H. Hahn
Address correspondence to Nadia R. Roan, roann@urology.ucsf.edu.
Supplemental material for this article may be found at http://dx.doi.org/10.1128/JVI.00269-14.

doi:10.1128/JVI.00269-14

cells (8), similar to the mechanism by which semen-derived enhancer of viral infection (SEVI) amyloids (9) promote viral infectivity. Amyloidogenic SEM peptides with junctions corresponding to PSA cleavage sites (4) that range in length from 40 to 63 amino acids form amyloid fibrils that are sufficient to enhance HIV infection over 30-fold *in vitro* (8). Importantly, whereas semen from healthy individuals markedly enhances HIV infection *in vitro* (8–16), semen samples naturally lacking SEMs due to ejaculatory duct obstruction (EDO) fail to enhance HIV infectivity (8). As amyloids derived from the SEMs have also been detected within the seminal vesicles of men, these fibrils may form even before semen emission (17).

As liquefaction is one of the characteristic properties of human semen, we set out to determine how this natural process affects the ability of semen to enhance HIV infection. Because the previously identified amyloidogenic SEM fragments contain internal PSA cleavage sites, PSA could, in theory, further cleave the amyloids formed from these peptides, which may affect virus-enhancing activity. In the present study, we demonstrate that semen progressively loses virus-enhancing activity during prolonged periods of liquefaction. We identify a short, naturally occurring amyloidogenic SEM fragment [residues 86 to 107 of SEM1, or SEM1(86–107)] whose levels correlate with both the changes in virus-enhancing activity during prolonged liquefaction and the variability in virus-enhancing activity between semen samples from different donors. This sequence, which shares the same amyloidogenic core as the previously identified SEM amyloids (8), forms amyloids that potently enhance HIV infection. We further provide evidence for the presence of endogenous SEM1(86-107) amyloids in semen and, using bioinformatics and biochemical approaches, show that the amyloidogenic potential of this peptide is conserved in great apes. These results identify SEM1(86-107) as a key factor in semen that enhances HIV infection and suggest an evolutionarily conserved function for amyloidogenic peptides in primate semen.

MATERIALS AND METHODS

Semen and seminal vesicle samples. Deidentified semen samples were obtained from the University of California, San Francisco (UCSF) Fertility Clinic and the Kinderwunschzentrum (Ulm, Germany) under protocol CHR 11-06115. Protocols for the use of human semen were approved by the Committee on Human Research at UCSF.

(i) Fresh samples. For analysis during the early time points of semen liquefaction, fresh ejaculate was collected and incubated at room temperature. After 10 min, when the ejaculate liquefied sufficiently for pipetting, an aliquot was added to HIV-1 and immediately tested for its effects on HIV infection in TZM-bl cell cultures (described below). Aliquots of this ejaculate were tested at the indicated times following initiation of liquefaction.

(ii) Frozen samples. To generate a pooled SF stock solution, 20 deidentified semen samples from healthy donors were allowed to liquefy for 2 h at room temperature and were then frozen at −20°C. All samples were then thawed simultaneously, pooled, and centrifuged at 1,500 rpm for 30 min at 4°C to remove spermatozoa and debris. The supernatant was aliquoted, frozen at −20°C, and used as the stock solution of SF. To determine whether extending the liquefaction period affects the ability of SF to enhance HIV infection, the stock was thawed, diluted 5-fold with phosphate-buffered saline (PBS) in the absence or presence of the protease inhibitor 4-(2-aminoethyl)benzenesulfonyl fluoride hydrochloride (AEBSF; 5 mM; Sigma-Aldrich, St. Louis, MO), and incubated for an additional 0.5, 2, 4, 8, or 24 h at 37°C before being frozen. When the entire time course was completed, all samples were thawed and tested simultaneously for the ability to enhance HIV infection of TZM-bl cells. Of note, these incubation times indicate the liquefaction time in addition to the 2 h of liquefaction before the SF stock solution was generated.

Seminal vesicle fluid was aspirated from the seminal vesicles of men with prostate cancer at the time of radical prostatectomy under protocol CHR 10-05134. Men were excluded if any pathological evidence of prostate cancer was noted within the seminal vesicles.

Peptides and fibrils. All peptides of semen-derived sequences were chemically synthesized by Celtek Peptides (Nashville, TN) or CPC Scientific (Sunnyvale, CA) and dissolved in PBS (pH 7.0) at a concentration of 2.5 mg/ml. SEM(86-107) sequences are shown in Table 1. Sequences not listed in Table 1 were those of SEM1(68-85) (TYHVDANDHDQSRKS QQY) and SEM2(93-109) (ATKSKQHLGGSQQLLNY) and the *Otolemur garnettii* repeat sequence (KTPQQQASQVTVV). To accelerate the nucleation of fibril formation, all peptide samples were agitated for 12 h in PBS at 37°C and 1,400 rpm in an Eppendorf Thermomixer, unless otherwise indicated. Agitation served to facilitate *ex vivo* fibril formation (18). Amyloid formation was confirmed by thioflavin T (ThT) and electron microscopy (EM) analyses.

TZM-bl infectivity assays. Infectivity assays were performed essentially as described previously (8, 14). 293T cells were transfected with CCR5-tropic 81A proviral DNA by Fugene (Promega, Madison, WI) and assayed for $p24^{Gag}$ content by enzyme-linked immunosorbent assay (ELISA; Perkin-Elmer, Waltham, MA). The supernatant was diluted to 100 ng/ml of $p24^{Gag}$ and treated for 5 min with semen, SF, or peptide/amyloid at the indicated pretreatment concentrations. Treated virions (20 μl) were added to 10^4 TZM-bl cells (280 μl). To minimize the toxic effects caused by prolonged exposure of SF to target cells, the medium was replaced after 2 h, and infection was assayed 3 days later by quantitating β-galactosidase activity (Gal-Screen kit; Life Technologies, Carlsbad, CA). Background signals obtained from uninfected cells were subtracted from the values obtained with infected cells.

Viral fusion assays. BlaM-Vpr chimeric CCR5-tropic HIV-1 81A was produced by Fugene reagent (Promega)-mediated cotransfection of 293T cells with CCR5-tropic 81A proviral DNA (20 μg), pCMV-BlaM-Vpr (6 μg), and the pAdvantage vector (2 μg), using methods previously described (19). Two days later, the virus-containing supernatant was filtered through 0.22-μm-pore-size Steriflip filter units (Millipore, Billerica, MA) to remove cellular debris and then aliquoted for storage at −80°C. Viral titers were measured by an anti-$p24^{Gag}$ ELISA (Perkin-Elmer). To examine HIV-1 fusion to target cells, we performed a virion fusion assay (19). BlaM-Vpr-containing 81A virions (170 ng/ml $p24^{Gag}$) were preincubated with SEM1(86-107) fibrils (10 to 200 μg/ml) or the appropriate negative control for 1 h at 37°C and then diluted 5-fold upon addition to 10^6 peripheral blood lymphocytes (PBLs) purified from buffy coats. Fusion was allowed to occur for 4 h at 37°C, after which target cells were washed once in CO_2-independent medium and loaded with CCF2-AM dye according to the manufacturer's directions (Life Technologies). After two washes, cells were resuspended in 200 μl of CO_2-independent medium supplemented with 10% fetal bovine serum (FBS) and 2.5 mM probenecid (Sigma-Aldrich), a nonspecific inhibitor of anion transport. The plate was sealed and incubated for 16 h at room temperature, washed once with PBS supplemented with 1% FBS and 2 mM EDTA, and then immunostained with CD4-phycoerythrin-Cy7 and CD3-allophycocyanin-Cy7 (BD Biosciences, San Jose, CA) to allow gating of $CD4^+$ T cells. Cells were then fixed overnight in 2% paraformaldehyde, and fluorescence-activated cell sorting (FACS) was carried out using a BD LSRII flow cytometer. FlowJo software (TreeStar, Ashland, OR) was used for data analysis. Results were derived from gating on live, $CD3^+$ $CD4^+$ cells.

Western blot analysis of SF. The equivalent of 0.2 to 1 μl of SF was loaded onto 12.5% Criterion Tris-HCl polyacrylamide gels (Bio-Rad, Hercules, CA). Proteins were transferred onto nitrocellulose iBlot membranes (Life Technologies, Grand Island, NY) and blocked with PBS in the presence of 5% milk and 0.1% Tween 20. Commercial antibodies against albumin and lactoferrin were purchased from Sigma-Aldrich. Custom-made antibodies against SEM amyloids (anti-S1) were described previ-

TABLE 1 SEM1(86-107) and SEM2(86-107) sequences used in this study[a]

A. SEM1(86–107)

Name	Sequence
Human SEM1(86–107)	**DLNALHKTTKSQRHLGGSQQLL**
Human SEM1(86–107) L100Q	DLNALHKTTKSQRHQGGSQQLL
P. troglodytes, P. paniscus (1), P. abelii, P. pygmaeus Q97E	DLNALHKTTKSERHLGGSQQLL
P. paniscus (2)	DLNALPKTTKSERHLGGSQQLL
G. gorilla	DLNALHETTKSERHLGGSQQLL
H. klossii	DLNAQHKMTKSERHLGGSQQLL
P. anubis	YSDAQHKTTKSEQHLRGSKELL
M. mulatta	YSNAQHKTTKSEQHLRGSQELL

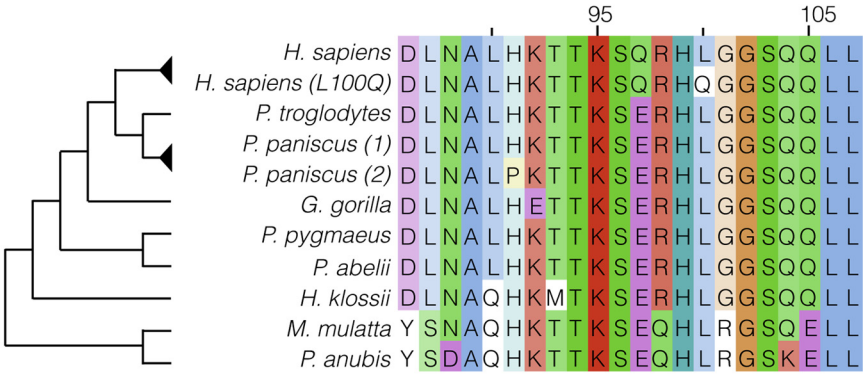

B. SEM2(86–107)

Name	Sequence
Human SEM2(86–107)	**DLNALHKATKSKQHLGGSQQLL**
G. gorilla	**DLNALHKATKSKQHLGGSQQLL**
P. troglodytes, P. paniscus	**DLNALHKVTKSKQHLDGSQQLL**
P. abelii, P. pygmaeus	**DLNALHKTRKSKQHLGGSQELL**
P. anubis	**YLNAQHKTTKSEQHLGRSQRLL**
C. guereza	**DLNAQHKTTKSEQHLGRSQRLL**
N. leucogenys	**DLNAQHKTTKSKQHLGGSQELL**
H. klossii, H. lar	**DLNAQHKMTKSKQHLGGSQELL**
M. mulatta, M. nemestrina	**YLNAQHKTTKSKQHLRRRQRLL**

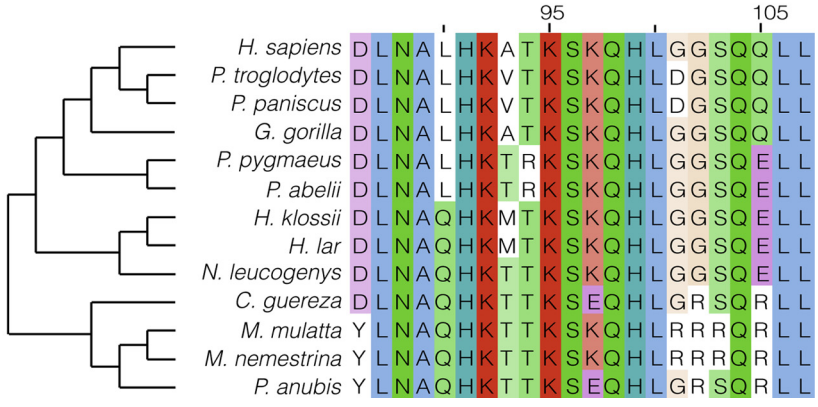

[a] (A) SEM1(86-107) sequences. (Top) NHP sequences are identified by primate origin, and differences from the common human SEM1(86-107) sequence are highlighted in red. Note that the sequences from *P. troglodytes*, *P. abelii*, *P. pygmaeus*, and a *P. paniscus* variant are identical and are referred to as Q97E due to a single amino acid difference relative to the common human SEM1(86-107) sequence. (Bottom) Sequences presented in the context of phylogenetic trees showing evolutionary relationships between species. (B) SEM2(86-107) sequences. (Top) Differences in the SEM2(86-107) sequence from the dominant human SEM1(86-107) sequence are highlighted in green, and differences in the NHP SEM2(86-107) sequences from the human SEM2(86-107) sequence are highlighted in red. Note that the SEM2(86-107) sequence from humans is identical to that of *G. gorilla*. (Bottom) Sequences presented in the context of phylogenetic trees showing evolutionary relationships between species. For the bottom parts of both section A and section B, differences in amino acid residues are highlighted by color according to the default ClustalX color scheme used by Jalview software.

ously (8). Primary antibodies were used at a dilution of 1:1,000 to 1:40,000, and horseradish peroxidase-conjugated secondary antibodies were used at a final dilution of 1:5,000. Immunoblots were developed using a Western Lightning ECL kit (PerkinElmer).

PSA substrate assay. The PSA substrate methyl-*O*-Suc-Arg-Pro-Tyr-*p*-nitroanilide was synthesized by CPC Scientific. Pooled SF stock was diluted to a concentration of 0.4% in PBS and incubated at 37°C with 0.4 mM substrate in the presence or absence of 5 mM AEBSF. Relative PSA activity was monitored by recording the absorbance at 405 nm on a spectrophotometer.

Mass spectrometry (MS). SF samples, generated as described above, were incubated at 37°C for the amounts of time indicated below in the absence or presence of 5 mM AEBSF and desalted with a ZipTip C_{18} pipette tip (Millipore). The desalted samples were fractionated on a monolithic column (inner diameter, 200 μm; length, 5 cm; Dionex, Sunnyvale, CA) on an Ultimate 3000 (Dionex) liquid chromatography (LC) system. A 20-min gradient, in which the percentage of phase B (80% acetonitrile [ACN], 0.05% trifluoroacetic acid [TFA]) was linearly increased from 0% to 80% at a flow rate of 2.5 μl/min, was used. The LC fractions were mixed with 5 mg/ml α-cyano-4-hydroxycinnamic acid (CHCA), the matrix for matrix-assisted laser desorption ionization (MALDI) mass spectrometry (MS), and spotted onto a blank stainless MALDI plate (Applied Biosystems [AB] Sciex, Foster City, CA) using a SunCollect spotter (SunChrom, Friedrichsdorf, Germany). A final concentration of 40 fmol/μl of [Glu^1]fibrinopeptide B (Glu-fib; *m/z* 1,570.677 Da) was spiked into the MALDI matrix for internal mass calibration. MS analyses of the MALDI plate were carried out on a 4800 MALDI-time of flight (TOF)/TOF analyzer (AB Sciex). MS and tandem MS (MS/MS) data were acquired in batch mode using 4000 Series Explorer software (AB Sciex). Peptides were identified by matching the MS/MS data against the MS/MS data for all human proteins in the Swiss-Prot database (release of 9 May 2011) using ProteinPilot software (version 4.0, revision 148085; AB Sciex). Manual inspection of the MS/MS spectrum was performed for SEM1(86-107) and SEM1(435-448) to confirm their identification. The presence of SEM1(86-107) in the insoluble fraction of SF was confirmed by pelleting the SF stock in an Eppendorf 5417R tabletop centrifuge (1,400 rpm, 5 min), dissolving the pellet in 0.5% HCl, and analyzing for the presence of SEM1(86-107) by MS/MS.

For monitoring SEM1(86-107) degradation in fresh semen, fresh ejaculates were incubated at 37°C for 1, 3, 5, or 8 h in the absence or presence of 5 mM AEBSF, desalted using a ZipTip C_{18} pipette tip (Millipore), and analyzed by electrospray ionization (ESI) LC-MS/MS. In brief, desalted samples were separated by a home-packed C_{18} reverse-phase column on a nano-LC Ultra 2D Plus system (Eksigent, Dublin, CA). A linear gradient, in which the percentage of phase B (2% ACN, 0.1% formic acid [FA]) was increased from 0 (at 0 min) to 40% (at 60 min) with a flow rate of 600 nl/min, was used. The total LC run time was 80 min. MS data were acquired using an LTQ Orbitrap Velos mass spectrometer (Thermo Scientific, Rockford, IL). Xcalibur Qual Browser software was used to process the raw MS data. The identity of SEM1(86-107) was confirmed by manual inspection of the MS and MS/MS data. Similar ESI LC-MS/MS methods were used to identify SEM2(93-109) from seminal vesicle fluid from three individual donors.

Absolute quantitation of SEM1(86-107) in semen from 19 donors was performed using an isotopic labeling-assisted MS strategy. Semen from 19 donors was allowed to liquefy for 2 h and then frozen. The samples were thawed simultaneously, and 50 μl of each sample was spiked with 100 μg/ml of a ^{13}C- and ^{15}N-labeled SEM1(86-107) peptide (Thermo Fisher Scientific, Rockford, IL), whose mass is 7 Da higher than that of the unlabeled counterpart. The samples were then desalted using ZipTip C_{18} pipette tips (Millipore), and native peptides were eluted stepwise with 30% and 40% ACN and 0.1% TFA. The eluates were spotted onto a MALDI target (Waters, Milford, MA) and analyzed by MALDI MS using a SYNAPT G2 HDMS high-definition MS system (20) equipped with a MALDI ion source and a Triwave ion mobility separator. The mobility separator allowed gas-phase separation of peptides whose MS peaks overlapped that of SEM1(86-107). Details on the quantitation of SEM1(86-107) by ion mobility MS (IMS) (20) will be described in a separate report. Briefly, IMS and MS/MS data were acquired in the mobility TOF mode. The extraction of IMS data that correspond to data for SEM1(86-107), whose sequence was verified by MS/MS, produced MS spectra of the unlabeled and labeled peptides. The ratios of the MS peak intensities of unlabeled versus labeled SEM1(86-107) were calculated, and the absolute level of the unlabeled peptide in each sample was determined from those ratios. Correlations between the levels of SEM1(86-107) and the virus-enhancing activity of individual semen samples were then assessed using Prism software (Irvine, CA).

To examine the cleavage of SEM1 protein by purified PSA, SEM1 protein was expressed and purified in *Escherichia coli* using a published plasmid construct (rSEMG1$^{24-283}$ in pET-100D/TOPO) and purification scheme (21). Following purification on a nickel column, SEM1 was stored in 4 M urea. A final concentration of 2.5 mg/ml of SEM1 was incubated with PSA (1.6 mg/ml; Abcam, Cambridge, MA) at 37°C for 0 h, 3 h, 8 h, 24 h, 3 days, or 7 days. The time course samples were then desalted using ZipTip C_{18} pipette tips (Millipore) and eluted with 50% ACN–0.1% TFA. The eluates were analyzed by MALDI MS using the SYNAPT G2 HDMS high-definition MS system.

Virus pulldown assay. The virion binding assay was conducted using methods similar to those previously described (10). Briefly, 81A virions (100 ng/ml p24^{Gag}) were incubated with peptide or fibrils (100 μg/ml) for 3 h at 37°C. The samples were then centrifuged at 13,000 rpm for 10 min, and HIV levels in the supernatant and pellet were assayed with an anti-p24^{Gag} ELISA kit (Perkin-Elmer). Results are reported as the percentage of p24^{Gag} in the pellet relative to the total p24^{Gag} content.

ThT binding. Peptides were added to 5 μM ThT (Sigma-Aldrich) in PBS at a concentration of 125 μg/ml. Increases in fluorescence (excitation, 440 nm; emission, 482 nm) were assayed in triplicate with a Perkin-Elmer Ls-5B luminescence spectrometer and an Enspire plate reader.

EM. Amyloid fibrils were prepared as described previously (22) and examined at 80 kV in a JEOL 1230 electron microscope. Representative fields were photographed with an Ultrascan USC1000 digital camera (Gatan, Pleasanton, CA). For immunogold labeling of fibrils, synthetic SEM1(86-107) fibrils or semen samples were adsorbed onto Formvar-coated grids and then blocked with 5% bovine serum albumin (BSA) in PBS for 15 min. Grids were then incubated with preimmune or postimmune serum from rabbits immunized with SEM1(86-107) fibrils (serum was custom produced by Pocono Rabbit Farms, Canadensis, PA) diluted 1:20 in PBS. Samples were then incubated with 10-nm gold-conjugated antirabbit antibody (Sigma-Aldrich) for 1 h in a water-saturated chamber. After rinsing three times with PBS and distilled water, the grids were stained using 2% uranyl acetate. Immunogold-labeled grids were examined using a JEOL JEM 1400 transmission electron microscope equipped with a charge-coupled-device camera operated at an accelerating voltage of 120 kV.

Confocal microscopy. For imaging the binding of SEM1(86-107) fibrils to virions, Gag-enhanced yellow fluorescent protein (EYFP) virions were produced by transfection of 293T cells with murine leukemia virus (MLV) Gag-EYFP and MLV-Gag-Pol expression plasmids using the calcium chloride method as described previously (23). Preformed SEM1(86-107) amyloid fibrils (final concentration, 50 μg/ml) were stained with a ProteoStat amyloid plaque detection kit (ENZ-51038–K040; Enzo Life Sciences, Germany) and then incubated with EYFP-tagged virions for 15 min at room temperature. Controls included SEM1(86-107) fibrils in the absence of virions and virions in the absence of the fibrils. Images were acquired with an LSM710 confocal microscope (Zeiss, Germany). ProteoStat dye was excited by a 561-nm laser line, and the emission was collected using an MBS 458/561 beam splitter. EYFP was excited by a 514-nm laser line, and the corresponding emission was collected using MBS 458/514 beam splitters. All the images were taken with the pinhole set to 1 airy unit and a Plan-Apochromat ×63 (numerical aperture, 1.40) oil objective lens.

Image acquisition and postacquisition brightness/contrast adjustment were done with Zen-2010 software (version 6; Zeiss).

For imaging of endogenous semen amyloids, liquefied ejaculate samples (100 μl) were mixed with 0.5% fish skin gelatin in PBS, and the mixture was incubated for 3 to 4 h at 4°C with preimmune or postimmune serum from rabbits immunized with SEM1(86-107) fibrils (serum was custom produced by Pocono Rabbit Farms). The antibody-amyloid complexes were pelleted at 13,000 rpm for 10 min, washed twice with PBS, and then pelleted. The pellet was dissolved in 0.5% fish skin gelatin containing PBS and treated with Alexa 488-conjugated secondary antibody for 3 h. The mixture was pelleted again, dissolved in PBS, and counterstained with ProteoStat dye. The Alexa 488 was excited by a 488-nm laser, the ProteoStat dye was excited by a 561-nm laser, and the respective emissions were collected using appropriate beam splitters. Plan-Apochromat ×63 (numerical aperture, 1.40) oil objective lenses on a Zeiss LSM710 confocal microscope (Oberkochen, Germany) equipped with Zen-Software were used to acquire images.

Nucleotide sequence accession numbers. Descriptions of the SEM protein sequences used in the bioinformatics analysis in this study are provided in Table 1.

RESULTS

Fresh semen exhibits potent virus-enhancing activity that decreases with extended liquefaction. We previously demonstrated that liquefied semen enhances HIV-1 infection (9, 14). The semen samples used in those studies were liquefied for a total of ~30 min and had undergone one freeze-thaw cycle before testing in infectivity assays. Here, we examined the effect of fresh ejaculates—which had never undergone any freeze-thaw cycles or other processing steps—on HIV-1 infection, as this would most closely mimic the activity of semen during natural transmission. We found that fresh ejaculates potently enhanced infection (Fig. 1A). Although enhancement activity was progressively reduced with increasing time of liquefaction, it remained significant even after 150 min (Fig. 1A).

The reduced ability of semen to enhance HIV infection is associated with degradation of SEM fragments. We next focused on the molecular events occurring during prolonged liquefaction that lead to the progressive decrease in the virus-enhancing activity of semen. Experiments with fresh ejaculates, like those used for Fig. 1A, are logistically challenging, owing to issues related to the timing of sample collection with assay initiation and the lack of sufficient material from a single ejaculate for multiple assays. To overcome these issues, we generated a stock solution of seminal fluid (SF) (see Materials and Methods) for the next set of assays, which provided ample material to study the effect of enhancing factors in the absence of spermatozoa and debris.

As shown in Fig. 1B, SF stocks incubated at 37°C progressively lost the ability to enhance HIV infection, consistent with the results from fresh ejaculates. To assess whether the decrease in semen's virus-enhancing activity was due to proteolysis during prolonged liquefaction, we tested whether protease inhibitors could prevent this reduction. Using 4-(2-aminoethyl)benzenesulfonyl fluoride hydrochloride (AEBSF), a serine protease inhibitor that blocks PSA activity in semen (4) (see Fig. S1A in the supplemental material), restored the HIV-enhancing activity of SF (Fig. 1C). Interestingly, the virus-enhancing activity after prolonged AEBSF treatment was increased compared to that of the starting SF stock, possibly due to the formation of new amyloids by amyloidogenic fragments protected from degradation in the presence of AEBSF. The addition of AEBSF in the absence of SF had no effect on HIV infection (see Fig. S1B in the supplemental material), indicating that the protease inhibitor was acting on factors in SF and not directly on HIV virions.

Western blot analyses were then used to determine whether the loss of virus-enhancing activity correlated with the degradation of SEMs. Samples described for Fig. 1C were immunoblotted with previously described antibodies generated against SEM1 fibrils (anti-S1) (8). Multiple SEM fragments were readily detected in the SF stock solution, and their levels gradually decreased over time (Fig. 1D, Mock). In comparison, degradation of SEM fragments was partially inhibited with AEBSF (Fig. 1D, AEBSF). Degradation of SEM fragments over time was specific, as levels of the semen proteins albumin and lactoferrin were constant over this time course (Fig. 1D, bottom two rows). Free Zn^{2+}, another inhibitor of PSA activity (24), also prevented SEM degradation and rescued HIV-enhancing activity (data not shown). These findings reveal that extended liquefaction, during which PSA cleaves SEM into progressively smaller fragments, coincides with the loss of the HIV-enhancing activity of SF.

The presence of SEM1(86-107), a PSA-generated fragment, correlates with virus-enhancing activity during extended liquefaction. To determine whether the levels of any amyloidogenic SEM fragments correlate with changes in virus-enhancing activity during extended liquefaction, we subjected the time course samples for Fig. 1C to LC-MS/MS analysis. Surprisingly, masses of peptides corresponding to the six SEM1 and SEM2 amyloidogenic fragments previously described (8) were not detected. Instead, we identified shorter SEM fragments, including a 2,445-Da fragment that corresponded to SEM1(86-107), a 22-mer subfragment derived from the previously reported amyloidogenic SEM1 peptides SEM1(45-107), SEM1(49-107), and SEM1(68-107) (8). SEM1(86-107) was present at the early stages of liquefaction but decreased in abundance by 8 h and was undetectable at 24 h. In contrast, in the presence of AEBSF, this fragment was readily detected at all time points (Fig. 2). To ensure that degradation of SEM1(86-107) was not an artifact specific to SF having undergone the freeze-thaw process, we confirmed that degradation of this peptide also occurred upon extended liquefaction of fresh semen in a manner rescued by AEBSF (see Fig. S2 in the supplemental material). Of note, not all SEM1 peptides exhibited degradation kinetics like SEM1(86-107), where levels corresponded with HIV-enhancing activity during extended liquefaction; in fact, some peptides increased in abundance as enhancing activity was lost (see Fig. S3 in the supplemental material).

SEM1(86-107) was, in fact, previously detected in SF by MS (8) but was not further analyzed because, at the time, the focus was on longer SEM peptides that overlapped with a region of SEM1 previously reported to be amyloidogenic in seminal vesicles (17). The inability of the present MS experiments to detect these longer SEM1 fragments in the SF stock is likely because of efficient PSA cleavage at internal sites within these peptides (4). Because the degradation kinetics of SEM1(86-107) correlated with reduced virus-enhancing activity during extended liquefaction, we further studied SEM1(86-107) metabolism using purified components.

Previously, SEM1(86-107) was reported to be a cleavage product of PSA (4). We confirmed that purified PSA catalyzes the release of SEM1(86-107) from recombinantly expressed SEM1 protein (see Fig. S4A in the supplemental material). PSA rapidly catalyzed the generation of SEM1(86-107) from SEM1 between 0 and 8 h but, interestingly, began to degrade the released SEM1(86-

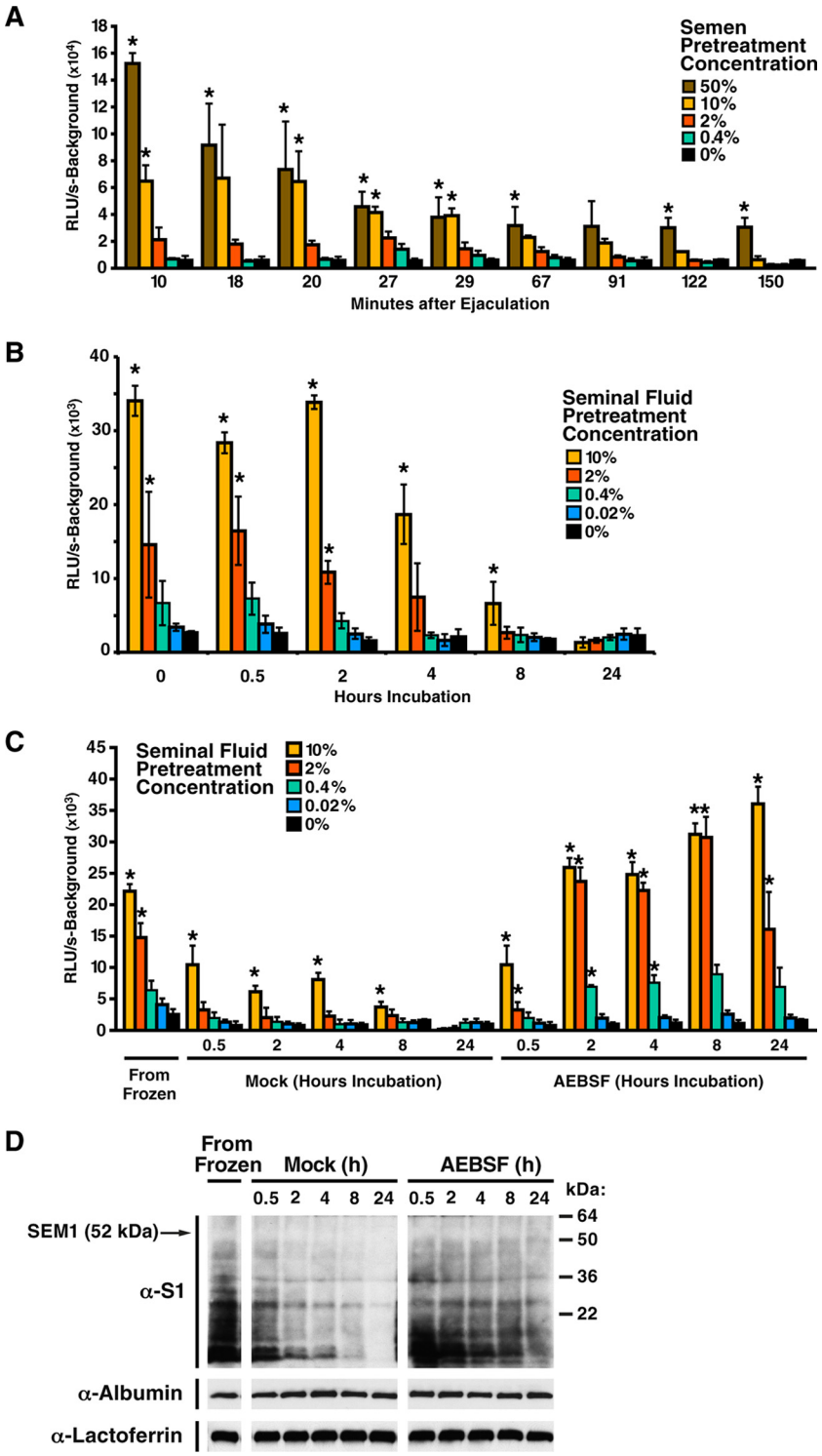

FIG 1 A progressive decrease in viral enhancement activity during extended liquefaction coincides with degradation of SEM fragments and can be rescued by AEBSF. (A) Fresh semen enhances HIV infection, but activity declines with increasing liquefaction time. Fresh ejaculate was liquefied for the indicated number of minutes before an aliquot was tested for the ability to enhance HIV-1 infection of TZM-bl cells. (B) To assess the effect of prolonged liquefaction on semen's ability to enhance HIV infection, a stock solution of SF was incubated for the indicated times and then tested for the ability to enhance HIV-1 infection of TZM-bl cells. (C) SF stock was incubated for the indicated periods of time in the absence (Mock) or presence of 5 mM AEBSF and then tested for HIV-enhancing activity. Panels A to C display the relative levels of infection in TZM-bl cells at 3 days postinfection, as assessed by luminescence. *, $P < 0.05$ (by one-way analysis of variance with a Bonferroni posttest) of each sample versus the no-semen control. The results in panels B and C are average values (means ± standard deviations) of triplicate measurements from 1 of 10 independent experiments with similar results. RLU/s, relative light units per second. (D) Samples for panel C were analyzed by Western blotting with the indicated primary antibodies. Full-length SEM1 (52 kDa) was not detected, suggesting that SEM cleavage had already been initiated in the SF stock.

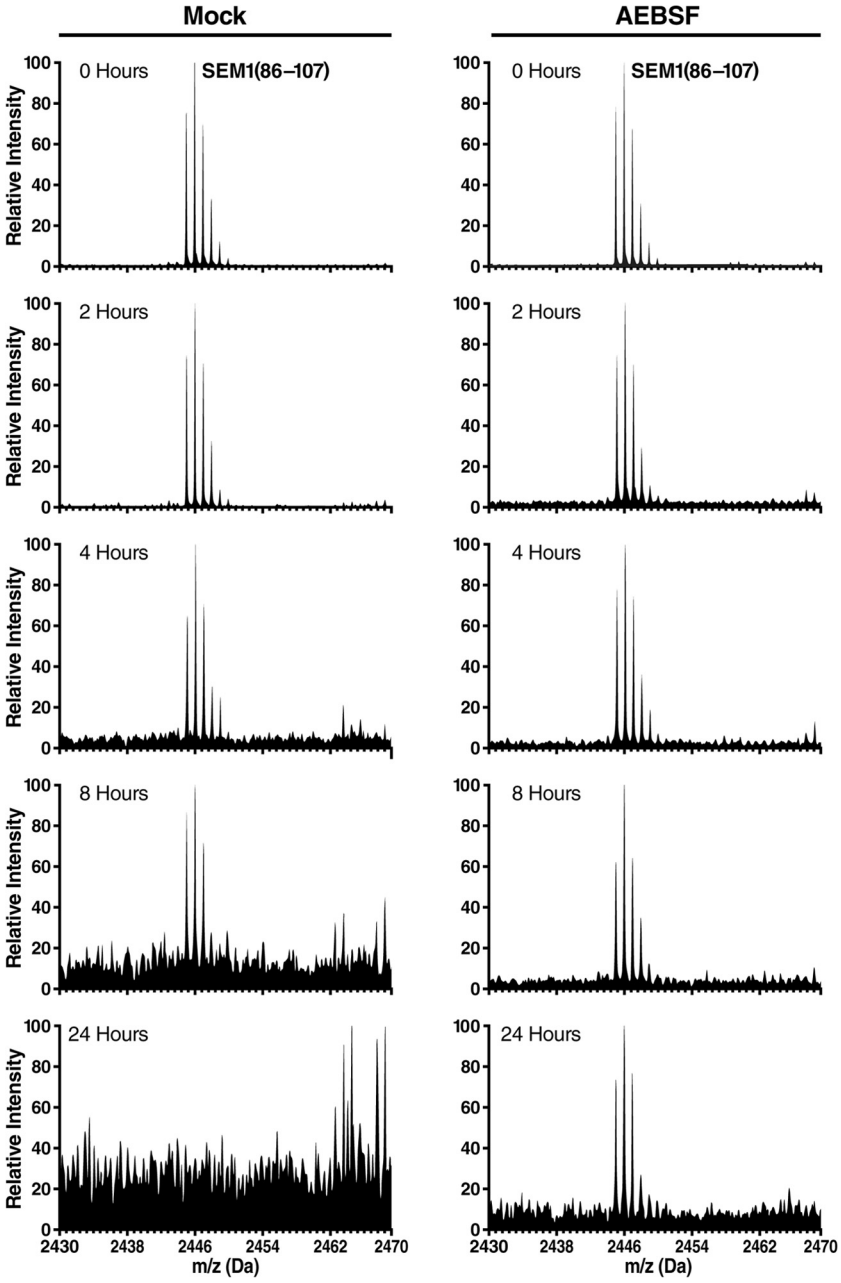

FIG 2 Endogenous SEM1(86-107) is degraded during prolonged liquefaction in a manner that is inhibited by AEBSF. Liquefied SF incubated for the indicated times at 37°C in the absence (Mock) or presence of 5 mM AEBSF was examined by MS. In the absence of AEBSF, SEM1(86-107) was detected between 0 to 8 h but not at 24 h, whereas in the presence of AEBSF, it was readily detected at all time points. All mass spectra shown were from a retention time of 11.0 to 11.7 min, when elution of SEM1(86-107) is maximum. The different peaks correspond to different naturally occurring isotopes of singly charged SEM1(86-107), with the first peak corresponding to the monoisotopic peak (m/z = 2,445.3 Da).

107) with further incubation, as reflected in a decrease in SEM1(86-107) levels at 24 h. By 3 days, the level of SEM1(86-107) was minimal, and by 7 days, the fragment was no longer detectable (see Fig. S4A in the supplemental material). These data confirm that SEM1(86-107) is a PSA-generated fragment and suggest that PSA had a weak ability to further cleave SEM1(86-107), although this activity was unfavorable and apparent only after 24 h.

SEM1(86-107) forms HIV-enhancing amyloid fibrils in a manner accelerated by SEM amyloids from seminal vesicles. SEM1(86-107) shares certain important properties with the other known HIV-enhancing amyloidogenic fragments (8, 9, 16). First, it is highly cationic (pI 9.99), more so than its parental SEM1(68-107) peptide (pI 8.16) (Fig. 3A) (8). Second, SEM1(86-107) contains a predicted amyloidogenic core GGSQQLL sequence at its C terminus, as determined by the ZipperDB amyloid prediction server (25). The same amyloidogenic core is also present in other amyloidogenic SEM peptides (8).

Because SEM1(86-107) catabolism coincided with the virus-

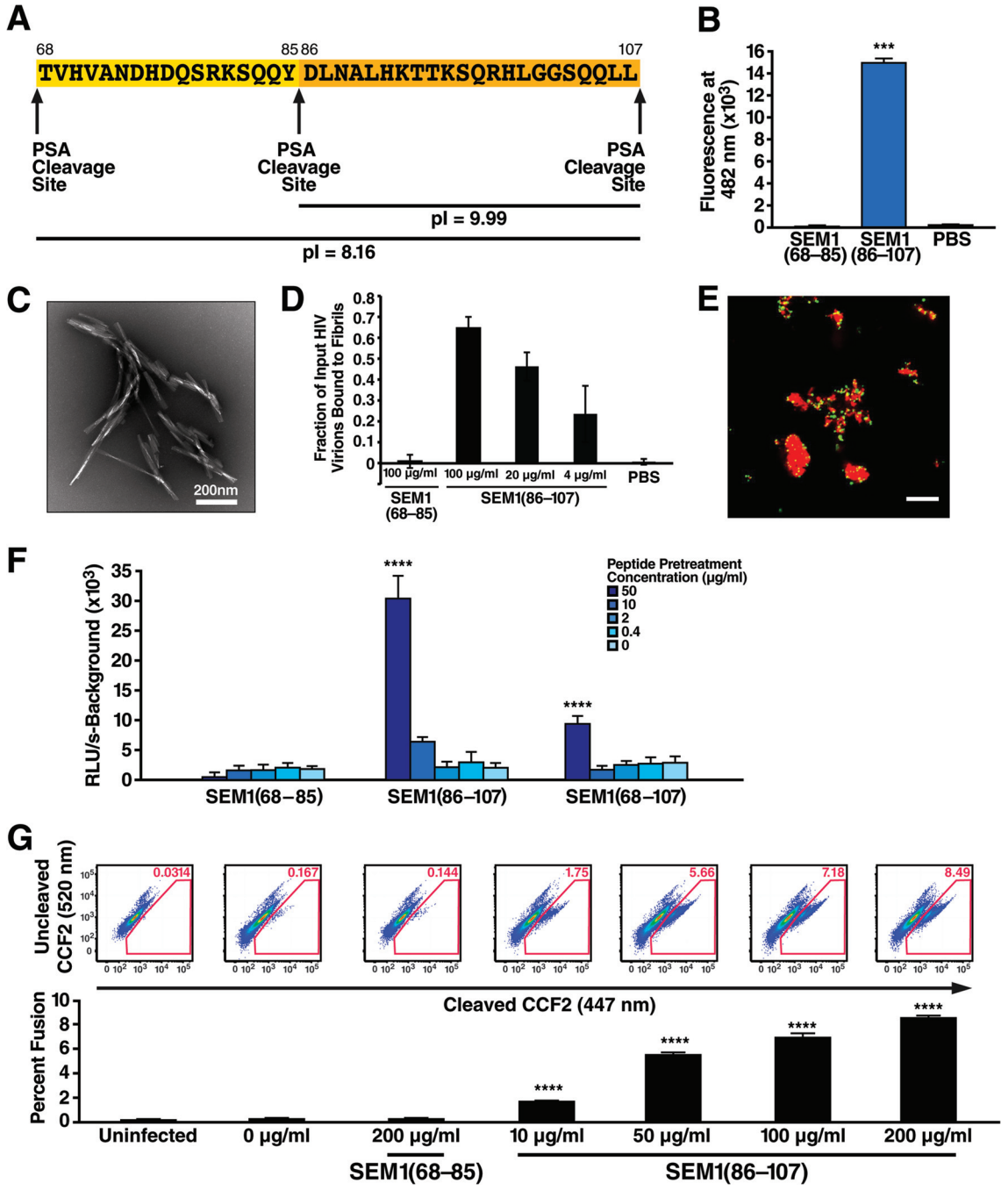

FIG 3 SEM1(86-107) forms amyloid fibrils that enhance HIV-1 infection. (A) The sequence of SEM1(86-107) in the context of its precursor SEM1(68-107), as described previously (8). Shown are the pIs and PSA cleavage sites, as delineated elsewhere (4). (B) Fluorescence measurements of the two PSA-released fragments of SEM1(68-107), SEM1(68-85) and SEM1(86-107), in the presence of the amyloid-binding agent ThT. ***, $P < 0.001$ relative to the PBS control (by two-tailed *t* test). (C) Representative EM image of SEM1(86-107) fibrils. (D) SEM1(86-107) fibrils directly bind HIV-1. The indicated concentrations of SEM1(86-107) fibrils or SEM1(68-85) as a negative control were incubated with HIV-1 81A virions, and the mixture was centrifuged. The absolute amounts of $p24^{Gag}$ in the pellet and supernatant were determined by ELISA and expressed as a fraction of the amount of input virions that pelleted. Results are representative of those from three experiments with similar results. (E) SEM1(86-107) fibrils bind fluorescently labeled virions. SEM1(86-107) fibrils (red) were incubated with Gag-EYFP virions (green) for 15 min and imaged by laser scanning confocal microscopy. Scale bar = 10 µm. (F) The relative abilities of SEM1(68-85), SEM1(86-107), and the precursor SEM1(68-107) to enhance HIV-1 infection were examined by infecting TZM-bl cells with HIV-1 treated with the indicated concentrations of peptide or fibrils. RLU/s, relative light units per second. Shown are average representative values (means ± standard deviations) of triplicate measurements from one of three independent experiments. ****, $P < 0.0001$ (by one-way analysis of variance with a Bonferroni posttest) of each sample versus the no-peptide control. (G) SEM1(86-107) but not SEM1(68-85) enhances the fusion of HIV-1 to primary $CD4^+$ T cells. PBLs were infected with BlaM-Vpr-containing 81A virions in the absence or presence of either 200 µg/ml SEM1(68-85) or 10 to 200 µg/ml SEM1(86-107), as indicated, and viral fusion was assessed by flow cytometry. (Top) Representative FACS plots for each condition, with the percentage of fused $CD4^+$ T cells indicated within the corresponding gates. (Bottom) Average fusion (± standard deviations) of triplicate measurements. ****, $P < 0.0001$ (by one-way analysis of variance with a Bonferroni posttest) for each sample versus the no-peptide control. Results are representative of data from one of three independent experiments.

enhancing activity of semen during extended liquefaction and this peptide was predicted to be amyloidogenic and highly cationic, we tested whether it could form virus-enhancing amyloid fibrils. We synthesized both SEM1(86-107) and SEM1(68-85), the other fragment released from SEM1(68-107) by PSA cleavage (Fig. 3A) (4). We found that SEM1(86-107), but not SEM1(68-85), formed amyloid fibrils, as assessed by thioflavin T (ThT) binding and electron microscopy (EM) (Fig. 3B and C). Because semen fibrils have been demonstrated to enhance HIV-1 infection by directly binding the virions (8, 9), SEM1(86-107) fibrils were tested for the ability to bind HIV-1. Using a fibril-virion binding assay previously described (10), we demonstrated that SEM1(86-107) fibrils, but not SEM1(68-85) fibrils, directly bind HIV-1 (Fig. 3D). The direct interaction between SEM1(86-107) fibrils and yellow fluorescent protein-labeled virions was confirmed by confocal microscopy (Fig. 3E; see Fig. S5 in the supplemental material).

Having demonstrated that SEM1(86-107) fibrils bind HIV-1, the fibrils were then tested for the ability to enhance HIV-1 infection of a reporter cell line. Whereas nonfibrillar SEM1(68-85) was inactive, SEM1(86-107) fibrils increased the infectivity of virus for TZM-bl cells (Fig. 3F). The ability of SEM1(86-107) fibrils to enhance HIV infection was superior to that of SEM1(68-107) fibrils (Fig. 3F), likely because the former has a higher isoelectric point than the latter (Fig. 3A). To determine whether SEM1(86-107) amyloids also enhanced HIV-1 infection of primary cells, $CD4^+$ peripheral blood lymphocytes (PBLs) were infected with CCR5-tropic HIV-1 81A packaged with a β-lactamase–Vpr reporter. Viral fusion was assessed by measuring the shift in fluorescence in target cells preloaded with the fluorescent compound CCF2, as previously described (19). As shown in Fig. 3G, SEM1(86-107) fibrils, but not the SEM1(68-85) peptide control, increased viral fusion to $CD4^+$ PBLs in a dose-dependent manner. These results suggest that, like SEVI (9), SEM1(86-107) amyloids increase the fusion of HIV-1 to cellular targets.

Seminal vesicles have been shown to harbor SEM-derived amyloids (17), and our data suggest that both virus-enhancing activity and the levels of SEM1(86-107) are high immediately postejaculation. We therefore postulated that seminal vesicle amyloids might seed and accelerate the polymerization of SEM fibrils immediately postejaculation. Consistent with published data (17), we detected fibrillar structures within seminal vesicle fluid (see Fig. S6A in the supplemental material). By MS analysis, we could not identify the SEM1(86-107) fragment within seminal vesicle fluid. This was expected, since PSA is not expressed in the seminal vesicles and, therefore, SEM1(86-107), a PSA-generated fragment, would not be predicted to be present in this gland. We did detect, however, SEM2(93-109), which shares an identical GG SQQLL amyloid core but is not a PSA-generated fragment (4). We found that seminal vesicle-derived SEM2(93-109) was amyloidogenic (see Fig. S6B in the supplemental material) and accelerated the formation of amyloids from monomeric SEM1(86-107) peptide (see Fig. S6C in the supplemental material). These findings support a model whereby SEM amyloid seeds in the seminal vesicle can facilitate the rapid polymerization of SEM1(86-107) fibrils at early times postemission, which may explain the high virus-enhancing activity of semen at this stage.

Endogenous SEM amyloids are present in semen, and absolute levels of endogenous SEM1(86-107) correlate with virus-enhancing activity. The data presented thus far suggest that SEM1(86-107) is present in semen and the synthetic peptide forms HIV-enhancing amyloids. To provide further evidence for the physiological relevance of SEM1(86-107) amyloids, we assessed whether endogenous SEM amyloids are present in semen. Endogenous amyloids in semen were imaged by EM using recently published techniques (23). Distinct fibrils with structures similar to those of synthetic SEM fibrils could be detected in semen. Immunogold labeling of these endogenous semen fibrils using antibodies generated against SEM1(86-107) amyloids revealed that these fibrils were reactive against anti-SEM1(86-107) (Fig. 4A). As a second approach to visualize endogenous SEM amyloids, we stained semen with ProteoStat, an amyloid-specific dye that binds endogenous semen amyloids (23). Costaining of semen with ProteoStat and antibodies generated against SEM1(86-107) revealed colocalization of anti-SEM1(86-107), but not preimmune serum, with endogenous amyloids (Fig. 4B). Of note, not all ProteoStat-stained structures reacted with anti-SEM1(86-107), suggesting that some endogenous amyloids are made up of other amyloidogenic peptides, for example, SEVI, as recently demonstrated (23). These data together suggest that endogenous SEM1(86-107) amyloids are present in semen.

To assess the levels of SEM1(86-107) naturally present in semen, we carried out quantitative IMS analysis of 19 semen samples from different donors. This analysis revealed that endogenous levels of SEM1(86-107) varied from 28 to 267 μg/ml (mean, 96.5 ± 71.3 μg/ml). Because 10 μg/ml SEM1(86-107) already significantly enhanced viral infection (Fig. 3), it can be concluded that physiologically relevant levels of SEM1(86-107) have potent virus-enhancing activity. Side-by-side comparison of the virus-enhancing activity of SF with that of the average physiological concentration of SEM1(86-107) fibrils (96.5 μg/ml) revealed that up to ~30% of the enhancing effects of SF can be accounted for by the concentrations of SEM1(86-107) present in this fluid (see Fig. S7 in the supplemental material). We further determined whether the absolute levels of SEM1(86-107) correlated with virus-enhancing activity. The 19 samples tested for endogenous SEM1(86-107) levels were tested for the relative ability to enhance HIV-1 infection of TZM-bl cells. As shown in Fig. 5, the relative levels of SEM1(86-107) in these samples significantly correlated with relative virus-enhancing activity. These findings suggest that SEM1(86-107) is likely a major contributor toward the ability of semen to enhance HIV infection.

Amyloid formation from SEM peptides is conserved in primates. SEM1(86-107) amyloids enhance HIV-1 infection, but these sequences are not likely to have evolved for this purpose. If, instead, SEM1(86-107) serves a physiological function, we would expect it to be conserved within the human population and across other species. To test this, we performed a comparative genomic analysis of the conservation of SEM1(86-107) in humans and nonhuman primates (NHPs) (Table 1A). According to dbSNP135, a human polymorphism database, a human variant of SEM1(86-107), rs61729393, codes for a L100Q substitution with a minor allele frequency of ~1.4%. The SEM1(86-107) ortholog in chimpanzees (*Pan troglodytes*) contains a single amino acid substitution, Q97E. The NHPs *Pan paniscus*, *Pongo abelii*, and *Pongo pygmaeus* share this genotype, whereas other NHPs have additional substitutions. Both human SEM1(86-107) variants consistently formed fibrils, as assessed by ThT fluorescence (Fig. 6A). The Q97E sequence present in *P. troglodytes*, *P. paniscus*, *P. abelii*, and *P. pygmaeus*

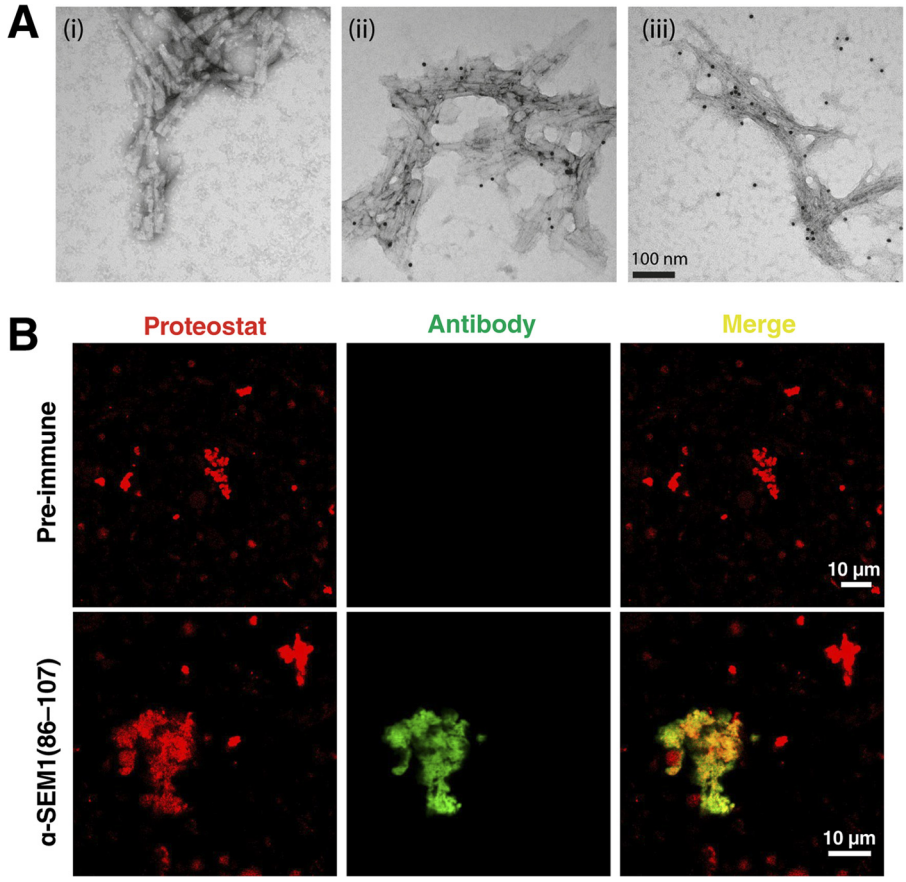

FIG 4 Endogenous semen amyloids bind anti-SEM1(86-107). (A) *In vitro*-generated SEM1(86-107) fibrils (i, ii) or fresh semen (iii) was treated with preimmune serum (i) or an anti-SEM1(86-107) antiserum (ii, iii), followed by incubation with a gold-conjugated secondary antibody, and then imaged by EM. (B) Detection of SEM1(86-107)-derived endogenous amyloid. Semen was stained with the amyloid dye ProteoStat (red) and either preimmune serum or anti-SEM1(86-107) (green). Colocalization is shown in yellow.

exhibited a positive ThT signal, as did the SEM1(86-107) orthologs from *Gorilla gorilla* and *Hylobates klossii* (Fig. 6A). EM confirmed that the ThT signal observed for the Q97E sequence corresponded to that of genuine amyloids, although interestingly, these fibrils were thinner than amyloids made up of human SEM1(86-107) (Fig. 6B).

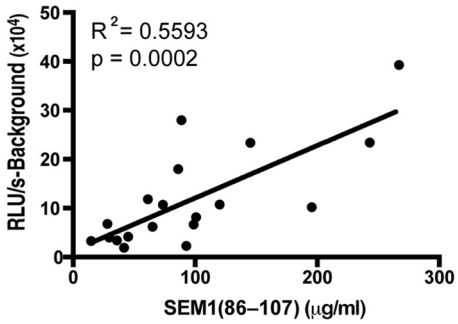

FIG 5 Endogenous levels of SEM1(86-107) correlate with virus-enhancing activity in semen samples from different donors. Semen samples from 19 different donors were liquefied for 2 h, spiked with isotopically labeled SEM1(86-107), and assessed by MALDI IMS for absolute concentrations of endogenous SEM1(86-107). In parallel, all samples were tested for virus-enhancing activity by pretreating HIV-1 with 10% (vol/vol) of each semen sample, diluting this mixture 15-fold upon addition to TZM-bl cells, and then quantitating infection 3 days postinfection by determining luciferase activity. RLU/s, relative light units per second. The graph shows a statistically significant correlation between SEM1(86-107) levels (in μg/ml, *x* axis) and infection levels in the presence of each semen sample (*y* axis).

Because some primates, including humans, have a second SEM protein, SEM2, we also assessed amyloid formation by primate orthologs of SEM2(86-107) (listed in Table 1B). ThT analysis of the SEM2(86-107) peptides revealed that the human SEM2(86-107), which is identical to the ortholog in *G. gorilla*, formed amyloid fibrils, as did the *P. troglodytes* and *P. paniscus* SEM2(86-107) orthologs. In contrast, the other NHP SEM2(86-107) orthologs did not (Fig. 6C). Interestingly, all SEM orthologs that formed amyloids enhanced HIV infection, whereas those that did not form amyloids lacked virus-enhancing activity (Fig. 6D and E). These data indicate that humans, *P. troglodytes*, *P. paniscus*, *P. abelii*, *P. pygmaeus*, *G. gorilla*, and *H. klossii* all have at least one SEM(86-107) sequence (from either SEM1 or SEM2) that forms amyloid fibrils capable of enhancing viral infection. These species are all great apes, with the exception of *H. klossii*, which is classified as a lesser ape. As such, species that harbor an amyloidogenic SEM(86-107) sequence are more closely related to each other than to other NHP species.

Some NHPs lack an ortholog of human SEM(86-107). We speculated that in such species, amyloidogenic sequences elsewhere in the SEM protein may substitute as a source of amyloids. We found that an example of this phenomenon may occur in the

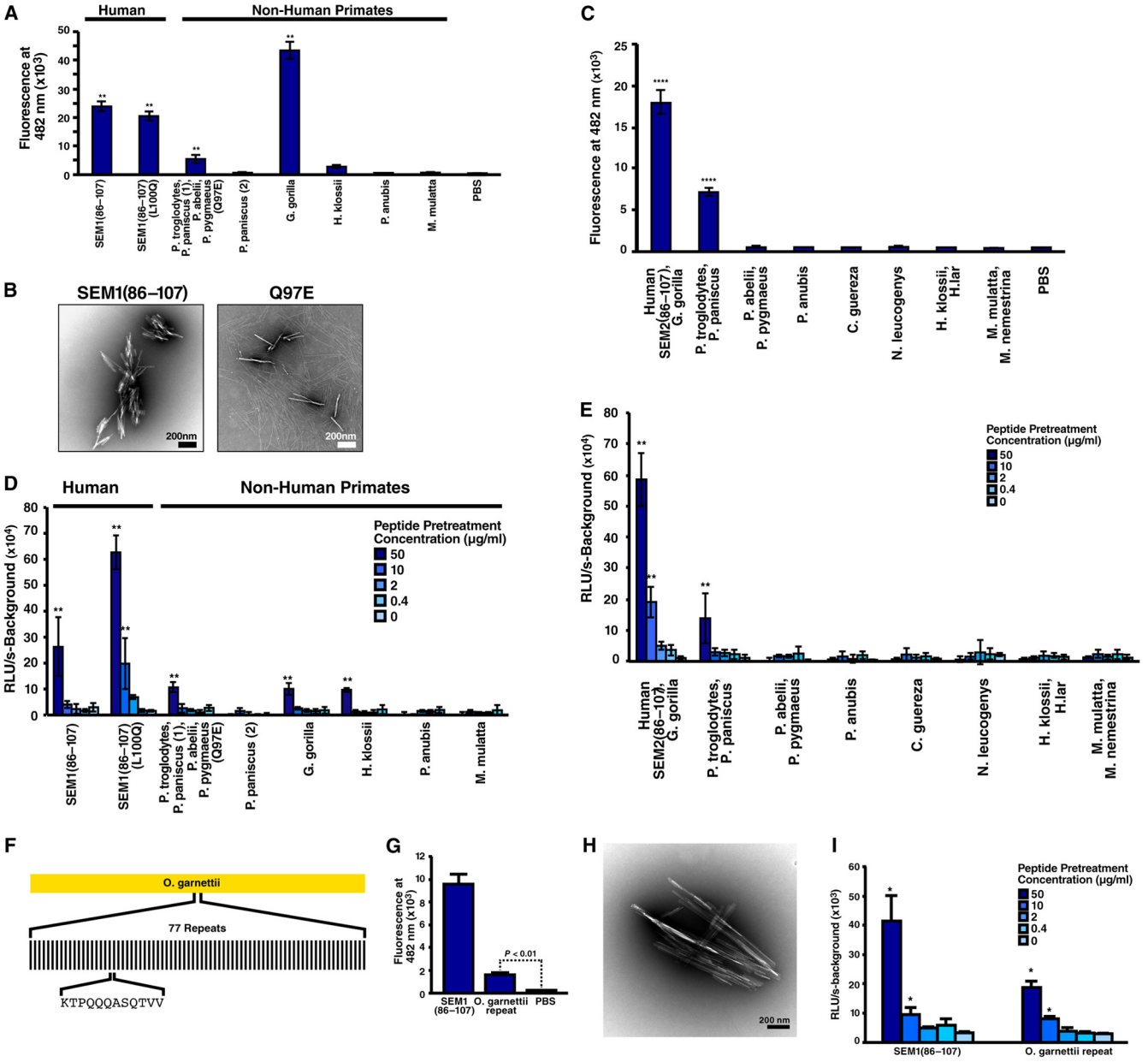

FIG 6 Amyloid fibril formation by SEM peptides is partially conserved in primates. (A) Human SEM1(86-107), the rare allelic SEM1(86-107) variant L100Q, and NHP orthologs of SEM1(86-107) were monitored for fibril formation by ThT fluorescence. **, $P < 0.01$ relative to the PBS control in a group-wise comparison (one-way analysis of variance with a Bonferroni posttest) of all samples. (B) Electron micrographs of SEM1(86-107) and Q97E samples. (C) Fibril formation by human SEM2(86-107) (which shares a sequence with the *G. gorilla* ortholog) and NHP orthologs of SEM2(86-107), assessed by ThT fluorescence. ****, $P < 0.0001$ relative to the PBS control in a group-wise comparison (one-way analysis of variance with a Bonferroni posttest) of all samples. (D, E) Peptide solutions for which the results are presented in panels A and C, respectively, were examined for their ability to enhance HIV-1 infection of TZM-bl cells. RLU/s, relative light units per second. **, $P < 0.01$ (by one-way analysis of variance with a Bonferroni posttest) of each sample versus the no-peptide control. (F) Schematic of the *O. garnettii* SEM2 gene, which lacks a sequence orthologous to human SEM(86-107). The 77-copy glutamine-rich-repeat insertion is shown, as is the sequence of one of the repeats. (G) The *O. garnettii* SEM2 repeat peptide was monitored for fluorescence in the presence of ThT. Human SEM1(86-107) and PBS served as positive and negative controls, respectively. (H) Representative EM image of *O. garnettii* SEM2 repeat fibrils. (I) The ability of SEM1(86-107) and *O. garnettii* SEM2 repeat amyloids to enhance HIV-1 infection was examined by infecting TZM-bl cells with HIV-1 isolates treated with the indicated concentrations of peptide. *, $P < 0.05$ (by one-way analysis of variance with a Bonferroni posttest) of the SEM1(86-107) and *O. garnettii* samples versus PBS. RLU/s, relative light units per second. Infectivity assay results are average representative values (means ± standard deviations) of triplicate measurements from one of at least three independent experiments.

lemur *Otolemur garnettii*, which lacks SEM1 but harbors one copy of SEM2. Although this SEM2 lacks a sequence orthologous to human SEM(86-107), it has a strikingly unusual ~3-kb insertion encoding 77 tandem copies of a cationic glutamine-rich repeat sequence (26) (Fig. 6F). As glutamine-rich sequences are commonly associated with amyloid formation (27) and the ZipperDB server predicted the repeated sequence to be highly amyloidogenic (data not shown), we tested whether this *O. garnettii* peptide forms amyloids. A chemically synthesized peptide corresponding to a single repeat (pI 8.75) formed amyloid fibrils and enhanced

viral infection in a dose-dependent manner (Fig. 6G to I). These results suggest that primates can have sources of cationic amyloidogenic SEM peptides lacking homology to human SEM1(86-107) and imply that the presence of cationic amyloids may be a general property of primate semen.

DISCUSSION

As semen is present during most cases of sexual HIV transmission, it is important to consider its effect on viral infectivity in efforts to limit the spread of HIV. Numerous studies have shown that semen enhances HIV infection *in vitro* under conditions minimizing the toxic effects of semen in cell culture (8–16). In this study, we set out to study the effect of liquefaction on semen's virus-enhancing activity. In doing so, we identified SEM1(86-107) as a naturally occurring, conserved PSA-generated amyloidogenic fragment whose presence correlates with the progressive loss of semen's virus-enhancing activity during prolonged liquefaction. SEM1(86-107) levels are maximal immediately postemission, when the virus-enhancing activity of semen is high, and this activity is progressively diminished during liquefaction in a manner that can be rescued by inhibiting the activity of serine proteases. Synthetic SEM1(86-107) peptide forms amyloid fibrils that directly interact with HIV-1 virions. Furthermore, amyloids in semen bind anti-SEM1(86-107) antibodies, suggesting that endogenous amyloids, which are present in human semen (23), are partly made up of SEM1(86-107) fragments. The relevance of SEM1(86-107) in semen's ability to enhance viral infection is further supported by our observation that endogenous levels of SEM1(86-107) correlate with virus-enhancing activity in a panel of 19 semen samples from different donors and that physiological levels of this fragment have a potent ability to enhance HIV infection of both cell lines and primary cells.

Our observation that semen exhibits maximal virus-enhancing activity immediately postemission, combined with the prior observation of SEM amyloids being present in seminal vesicles (17), is consistent with a model in which preformed seminal vesicle-derived amyloids facilitate the rapid polymerization of PSA-generated SEM1(86-107) into amyloid fibrils in semen. Supporting this model is our finding that seminal vesicle fluid harbors peptides that form amyloids capable of seeding the polymerization of SEM1(86-107) into fibrils. Once polymerized, SEM1(86-107) fibrils can facilitate HIV infection but, at the same time, are subjected to proteolysis by seminal proteases. The proteolytic activity of seminal proteases therefore appears to be responsible for both generating and, with sufficient time, degrading the peptide that forms the SEM1(86-107) fibrils. Thus, seminal proteases may be a double-edged sword, a factor that can both facilitate and destroy semen's virus-enhancing activity, depending on how long it is in contact with SEM. As such, microbicide strategies aimed at inhibiting the activity of seminal proteases to prevent the generation of SEM1(86-107) may, in fact, extend the window of opportunity for semen to enhance HIV infection. The identity of the protease(s) that degrades SEM1(86-107) is unknown. Although purified PSA degraded SEM1(86-107), it did so only at >24 h of treatment (see Fig. S3 in the supplemental material) and is therefore unlikely to be the primary SEM1(86-107)-cleaving protease. Given that degradation of SEM1(86-107) in semen is inhibited in the presence of a serine protease inhibitor, it is likely that the responsible protease(s) is another serine protease(s), such as the numerous kallikrein-related peptidases expressed in human semen (28–30).

The fact that semen loses virus-enhancing activity with time brings up the question of whether this activity is retained long enough to promote viral transmission in the *in vivo* setting. As shown in Fig. 1, SF retains virus-enhancing activity for over 8 h postemission. Because simian immunodeficiency virus can infect cells of the vaginal mucosa within 60 min of vaginal exposure (31), semen likely has ample opportunity to promote transmission within the genital mucosa. Besides the liquefaction period, the virus-enhancing activity of semen can also vary due to donor-dependent differences (8, 14) (Fig. 5), and even longitudinal samples isolated from the same donor can differ in the extent to which they enhance HIV infection (32). Whether differences in protease activity in these samples underlie this variability remains to be determined.

We found that amyloid formation occurred in all the human variants of SEM(86-107) and in at least one corresponding ortholog from *P. troglodytes*, *P. paniscus*, *P. abelii*, *P. pygmaeus*, *G. gorilla*, and *H. klossii* (Fig. 6). Apart from *H. klossii*, all of these species are classified as great apes. These data suggest that an ancestor of the great apes acquired an amyloidogenic SEM(86-107) sequence. Although the ability of SEM(86-107) to form amyloids appears to be somewhat limited to great apes, we predict that amyloidogenic peptides are generally present in the semen of all NHPs, given that multiple amyloid species are present in semen (9, 16). In support of this idea, the *O. garnettii* SEM protein lacks a sequence homologous to human SEM1(86-107) but contains a unique Gln-rich repeat sequence that forms cationic amyloid fibrils with properties similar to those of SEM1(86-107) fibrils, including the ability to enhance lentiviral infection. As no primary sequence homology exists between the *O. garnettii* repeat sequence and human SEM(86-107), this appears to be a case of convergent evolution. The NHP semen analysis in this study was limited to examining synthetic peptides, but future studies examining the constituents and structures of endogenous amyloids in semen from NHPs should be conducted to confirm whether semen amyloids are indeed conserved in primates. As the viscosity of NHP semen differs between species (semen from some primates, such as chimpanzees, forms a firm copulatory plug) (26), it would be intriguing to test whether the different amyloidogenic sequences in NHPs generate variant fibril structures that affect semen consistencies.

Why do multiple amyloidogenic peptides exist in semen? Amyloidogenic peptides from SEM1, SEM2, and prostatic acid phosphatase (the precursor protein for SEVI) could serve distinct functions and/or coassemble together to form heteromeric amyloids with different physical properties. Although the purpose of having multiple amyloidogenic semen peptides remains elusive, all the amyloidogenic semen peptides identified thus far (i) derive from abundant proteins whose expression is relatively specific for male reproductive organs and (ii) are cationic. These common features suggest that, while seemingly redundant, these proteins might serve an important physiological role, perhaps in reproduction. Intriguingly, semen from EDO patients lacks SEM and SEVI amyloids (8), and these patients are infertile. It will be vital to determine whether semen amyloids promote fertility, since if they do, such knowl-

edge would be an important consideration for any HIV microbicide strategy targeting these structures.

ACKNOWLEDGMENTS

We thank J. Wong for generating electron micrographs, M. O'Rand for providing the SEM1 protein expression construct, A. Holloway for bioinformatics analysis, A. L. Lucido for editorial assistance, J. Carroll and T. Roberts for assistance in preparing the figures, and S. Cammack and R. Givens for administrative assistance.

This work was supported, in whole or in part, by grant 5K12 DK083021-04 KURe, grant K99/R00 1K99AI104262, and Hellman Family Awards grants (to N.R.R.), grant 1PO1 AI083050 PPG and U.S. Department of Defense grant W81XWH-11-1-0562 (to W.C.G.), grant R01HD074511 (to N.R.R. and W.C.G.), the DFG and the Ministry of Science (to J.M.), the VW Stiftung (to J.M. and F.K.), DFG FA 456/10-1 (to M.F.), DFG US116/1– funding (to S.M.U., a fellow of the DFG Junior Research Academy OFFSPRing), and institutional funds from the Gladstone Institutes and a gift from the San Simeon Fund (to K.S.P.). The UCSF Sandler-Moore Mass Spectrometry Core Facility acknowledges support from the Sandler Family Foundation, the Gordon and Betty Moore Foundation, and NIH/NCI Cancer Center support grant P30 CA082103. We also acknowledge CFAR for funding for the Flow Core (P30 AI027763) and for H.L. (P30-AI027763).

The funders had no role in study design, data collection and analysis, decision to publish, or preparation of the manuscript.

REFERENCES

1. **de Lamirande E.** 2007. Semenogelin, the main protein of the human semen coagulum, regulates sperm function. Semin. Thromb. Hemost. **33:**60–68. http://dx.doi.org/10.1055/s-2006-958463.
2. **Taylor U, Rath D, Zerbe H, Schuberth HJ.** 2008. Interaction of intact porcine spermatozoa with epithelial cells and neutrophilic granulocytes during uterine passage. Reprod. Domest. Anim. **43:**166–175. http://dx.doi.org/10.1111/j.1439-0531.2007.00872.x.
3. **Lilja H, Oldbring J, Rannevik G, Laurell CB.** 1987. Seminal vesicle-secreted proteins and their reactions during gelation and liquefaction of human semen. J. Clin. Invest. **80:**281–285. http://dx.doi.org/10.1172/JCI113070.
4. **Robert M, Gibbs BF, Jacobson E, Gagnon C.** 1997. Characterization of prostate-specific antigen proteolytic activity on its major physiological substrate, the sperm motility inhibitor precursor/semenogelin I. Biochemistry **36:**3811–3819. http://dx.doi.org/10.1021/bi9626158.
5. **Koistinen H, Soini T, Leinonen J, Hyden-Granskog C, Salo J, Halttunen M, Stenman UH, Seppala M, Koistinen R.** 2002. Monoclonal antibodies, immunofluorometric assay, and detection of human semenogelin in male reproductive tract: no association with in vitro fertilizing capacity of sperm. Biol. Reprod. **66:**624–628. http://dx.doi.org/10.1095/biolreprod66.3.624.
6. **Kingan SB, Tatar M, Rand DM.** 2003. Reduced polymorphism in the chimpanzee semen coagulating protein, semenogelin I. J. Mol. Evol. **57:**159–169. http://dx.doi.org/10.1007/s00239-002-2463-0.
7. **Dorus S, Evans PD, Wyckoff GJ, Choi SS, Lahn BT.** 2004. Rate of molecular evolution of the seminal protein gene SEMG2 correlates with levels of female promiscuity. Nat. Genet. **36:**1326–1329. http://dx.doi.org/10.1038/ng1471.
8. **Roan NR, Muller JA, Liu H, Chu S, Arnold F, Sturzel CM, Walther P, Dong M, Witkowska HE, Kirchhoff F, Munch J, Greene WC.** 2011. Peptides released by physiological cleavage of semen coagulum proteins form amyloids that enhance HIV infection. Cell Host Microbe **10:**541–550. http://dx.doi.org/10.1016/j.chom.2011.10.010.
9. **Munch J, Rucker E, Standker L, Adermann K, Goffinet C, Schindler M, Wildum S, Chinnadurai R, Rajan D, Specht A, Gimenez-Gallego G, Sanchez PC, Fowler DM, Koulov A, Kelly JW, Mothes W, Grivel JC, Margolis L, Keppler OT, Forssmann WG, Kirchhoff F.** 2007. Semen-derived amyloid fibrils drastically enhance HIV infection. Cell **131:**1059–1071. http://dx.doi.org/10.1016/j.cell.2007.10.014.
10. **Roan NR, Munch J, Arhel N, Mothes W, Neidleman J, Kobayashi A, Smith-McCune K, Kirchhoff F, Greene WC.** 2009. The cationic properties of SEVI underlie its ability to enhance human immunodeficiency virus infection. J. Virol. **83:**73–80. http://dx.doi.org/10.1128/JVI.01366-08.
11. **Roan NR, Sowinski S, Munch J, Kirchhoff F, Greene WC.** 2010. Aminoquinoline surfen inhibits the action of SEVI (semen-derived enhancer of viral infection). J. Biol. Chem. **285:**1861–1869. http://dx.doi.org/10.1074/jbc.M109.066167.
12. **Bouhlal H, Chomont N, Haeffner-Cavaillon N, Kazatchkine MD, Belec L, Hocini H.** 2002. Opsonization of HIV-1 by semen complement enhances infection of human epithelial cells. J. Immunol. **169:**3301–3306. http://dx.doi.org/10.4049/jimmunol.169.6.3301.
13. **Hauber I, Hohenberg H, Holstermann B, Hunstein W, Hauber J.** 2009. The main green tea polyphenol epigallocatechin-3-gallate counteracts semen-mediated enhancement of HIV infection. Proc. Natl. Acad. Sci. U. S. A. **106:**9033–9038. http://dx.doi.org/10.1073/pnas.0811827106.
14. **Kim KA, Yolamanova M, Zirafi O, Roan NR, Staendker L, Forssmann WG, Burgener A, Dejucq-Rainsford N, Hahn BH, Shaw GM, Greene WC, Kirchhoff F, Munch J.** 2010. Semen-mediated enhancement of HIV infection is donor-dependent and correlates with the levels of SEVI. Retrovirology **7:**55. http://dx.doi.org/10.1186/1742-4690-7-55.
15. **Olsen JS, Brown C, Capule CC, Rubinshtein M, Doran TM, Srivastava RK, Feng C, Nilsson BL, Yang J, Dewhurst S.** 2010. Amyloid-binding small molecules efficiently block SEVI (semen-derived enhancer of virus infection)- and semen-mediated enhancement of HIV-1 infection. J. Biol. Chem. **285:**35488–35496. http://dx.doi.org/10.1074/jbc.M110.163659.
16. **Arnold F, Schnell J, Zirafi O, Sturzel C, Meier C, Weil T, Standker L, Forssmann WG, Roan NR, Greene WC, Kirchhoff F, Munch J.** 2011. Naturally occurring fragments from two distinct regions of the prostatic acid phosphatase form amyloidogenic enhancers of HIV infection. J. Virol. **86:**1244–1249. http://dx.doi.org/10.1128/JVI.06121-11.
17. **Linke RP, Joswig R, Murphy CL, Wang S, Zhou H, Gross U, Rocken C, Westermark P, Weiss DT, Solomon A.** 2005. Senile seminal vesicle amyloid is derived from semenogelin I. J. Lab. Clin. Med. **145:**187–193. http://dx.doi.org/10.1016/j.lab.2005.02.002.
18. **Giehm L, Otzen DE.** 2010. Strategies to increase the reproducibility of protein fibrillization in plate reader assays. Anal. Biochem. **400:**270–281. http://dx.doi.org/10.1016/j.ab.2010.02.001.
19. **Cavrois M, De Noronha C, Greene WC.** 2002. A sensitive and specific enzyme-based assay detecting HIV-1 virion fusion in primary T lymphocytes. Nat. Biotechnol. **20:**1151–1154. http://dx.doi.org/10.1038/nbt745.
20. **Kanu AB, Dwivedi P, Tam M, Matz L, Hill HH, Jr.** 2008. Ion mobility-mass spectrometry. J. Mass Spectrom. **43:**1–22. http://dx.doi.org/10.1002/jms.1383.
21. **Mitra A, Richardson RT, O'Rand MG.** 2010. Analysis of recombinant human semenogelin as an inhibitor of human sperm motility. Biol. Reprod. **82:**489–496. http://dx.doi.org/10.1095/biolreprod.109.081331.
22. **Hamilton RL, Jr, Goerke J, Guo LS, Williams MC, Havel RJ.** 1980. Unilamellar liposomes made with the French pressure cell: a simple preparative and semiquantitative technique. J. Lipid Res. **21:**981–992.
23. **Usmani S, Zirafi O, Muller JA, Sandi-Monroy NL, Yadav JK, Meier C, Weil T, Roan NR, Greene WC, Walther P, Nilsson KP, Hammarstrom P, Wetzel R, Pilcher CD, Gagsteiger F, Fandrich M, Kirchhoff F, Munch J.** 2014. Direct visualization of HIV-enhancing endogenous amyloid fibrils in human semen. Nat. Commun. **5:**3508. http://dx.doi.org/10.1038/ncomms4508.
24. **Jonsson M, Linse S, Frohm B, Lundwall A, Malm J.** 2005. Semenogelins I and II bind zinc and regulate the activity of prostate-specific antigen. Biochem. J. **387:**447–453. http://dx.doi.org/10.1042/BJ20041424.
25. **Goldschmidt L, Teng PK, Riek R, Eisenberg D.** 2010. Identifying the amylome, proteins capable of forming amyloid-like fibrils. Proc. Natl. Acad. Sci. U. S. A. **107:**3487–3492. http://dx.doi.org/10.1073/pnas.0915166107.
26. **Hurle B, Swanson W, Green ED.** 2007. Comparative sequence analyses reveal rapid and divergent evolutionary changes of the WFDC locus in the primate lineage. Genome Res. **17:**276–286. http://dx.doi.org/10.1101/gr.6004607.
27. **Rubinsztein DC, Carmichael J.** 2003. Huntington's disease: molecular basis of neurodegeneration. Expert Rev. Mol. Med. **5:**1–21. http://dx.doi.org/10.1017/S1462399403006549.
28. **Lundwall A, Brattsand M.** 2008. Kallikrein-related peptidases. Cell. Mol. Life Sci. **65:**2019–2038. http://dx.doi.org/10.1007/s00018-008-8024-3.
29. **Robert M, Gagnon C.** 1994. Sperm motility inhibitor from human seminal plasma: presence of a precursor molecule in seminal vesicle fluid and

its molecular processing after ejaculation. Int. J. Androl. **17:**232–240. http://dx.doi.org/10.1111/j.1365-2605.1994.tb01248.x.

30. **Emami N, Deperthes D, Malm J, Diamandis EP.** 2008. Major role of human KLK14 in seminal clot liquefaction. J. Biol. Chem. **283:**19561–19569. http://dx.doi.org/10.1074/jbc.M801194200.
31. **Hu J, Gardner MB, Miller CJ.** 2000. Simian immunodeficiency virus rapidly penetrates the cervicovaginal mucosa after intravaginal inoculation and infects intraepithelial dendritic cells. J. Virol. **74:**6087–6095. http://dx.doi.org/10.1128/JVI.74.13.6087-6095.2000.
32. **Hartjen P, Frerk S, Hauber I, Matzat V, Thomssen A, Holstermann B, Hohenberg H, Schulze W, Schulze Zur Wiesch J, van Lunzen J.** 2012. Assessment of the range of the HIV-1 infectivity enhancing effect of individual human semen specimen and the range of inhibition by EGCG. AIDS Res. Ther. **9:**2. http://dx.doi.org/10.1186/1742-6405-9-2.